Retrieval of developmental social memories requires activation of the adult-born granule cell-CA2 circuit in mice

Blake J. Laham, Isha R. Gore, Casey J. Brown, Elizabeth Gould
Princeton Neuroscience Institute, Princeton University, Princeton NJ 08544

Address correspondence to:
Elizabeth Gould PhD
Princeton Neuroscience Institute
Princeton University
goulde@princeton.edu
609-258-4483

Acknowledgments: This work was supported by the National Institutes of Health, NIMH 1R01 MH118631-01 to EG. The authors thank Samantha H. Wang for performing surgeries on PV-cre mice. The authors acknowledge Biorender for assistance with the figure schematics.

Abstract

Adult-born granule cells (abGCs) project to the CA2 region of the hippocampus, but no previous studies have assigned a behavioral function to this circuit. Here we show that abGC input to the CA2 is necessary for the retrieval of remote social memories. Ablation of abGCs impaired retrieval of developmental social memories, while this ability returned after new neurons were regenerated. Chemogenetic inhibition of projections from abGCs to the CA2 also temporarily prevented the retrieval of developmental memories. These findings were observed when abGCs were 4-6 weeks old, but not when they were 10-12 weeks old. We also found that abGCs are necessary for differential CA2 network activity, including theta-gamma coupling and sharp wave-ripples, in response to novel versus familiar social stimuli. Taken together, these findings suggest that abGCs are necessary for neuronal oscillations associated with discriminating between social stimuli, thus enabling remote memory retrieval.

Introduction

The earliest social memories arise as infants learn to recognize their first caregiver - most commonly, the mother. In humans, these early associations can be further strengthened by emotional valence and shared experiences as the child develops, forming memories of the mother that can last a lifetime (Fivush et al., 2011; Schaal et al., 2020). Mice form memories of their mothers during the first postnatal week (Laham et al., 2021). These memories last well into adulthood, with a reversal in social preference at the time of weaning (Laham et al., 2021); pups prefer investigating their own mothers over novel mothers, while adult offspring prefer investigating novel mothers to their own. One area known to be important for retrieval of these remote social memories is the hippocampal CA2 (Laham et al., 2021). The CA2 is also known to support short-term social memories of peers during development and in adulthood (Diethorn and Gould., 2023; Hitti and Siegelbaum, 2014; Laham et al., 2021; Smith et al., 2016). It is known that the CA2 receives afferent input from both mature and adult-born granule cells of the dentate gyrus (DG), but the functional relevance of this pathway remains entirely unexplored (Diethorn and Gould, 2023; Kohara et al., 2014; Llorens-Martin et al., 2015).

Results

abGCs project to inhibitory interneurons and pyramidal cells of the CA2 region

In the CA2, we verified adult-born granule cell (abGC) projections using 3R-Tau, a marker of abGC axons (Llorens-Martin et al., 2015), as well as mature granule cell projections using ZnT3, a marker of mature mossy fibers (Wenzel et al., 1997) (Figure 1a). We further determined that abGC projections to the CA2 preferentially innervate the soma and dendrites of PV+ interneurons labeled with cre-dependent AAV mCherry compared to pyramidal cells immunolabeled with PCP4 (Figure 1b-f), which mirrors abGC projection patterns to the CA3 (Restivo et al., 2015).

abGCs are necessary for retrieval, but not storage, of remote developmental memories

Previous studies have shown that abGCs participate in social recognition of recently encountered mice (Cope et al., 2020, Pereira-Caixeta et al., 2018), nonsocial memory retrieval (Tronel et al., 2015), and pattern separation (McHugh et al., 2022). However, whether inputs from abGCs to CA2 participate in the retrieval of remote social memories laid down during development, especially those formed long before abGCs were born, remains unexplored.

Hippocampal phase-amplitude coupling (PAC) and generation of sharp wave-ripples (SWRs) have been linked to novel experience, memory consolidation, and retrieval (Colgin, 2015; Fernandez Ruiz et al., 2019; Meier et al., 2020; Joo and Frank, 2018; Vivekananda et al., 2021). The DG is known to influence hippocampal theta-gamma coupling and SWRs (Bott et al, 2016; Meier et al., 2020), yet no studies have examined the influence of abGCs on these oscillatory patterns. Here we investigated whether abGCs support the retrieval of developmental social memories and contribute to socially relevant CA2 network activity.

Using the GFAP-TK transgenic mouse model in which abGCs are ablated upon valganciclovir (VGCV) administration (Snyder et al., 2011), we found that mice with normal levels of abGCs can discriminate between their own mother and a novel mother, similar to what has been observed in control mice (Laham et al., 2021). In contrast, those with abGC depletion lose this ability (Figure 1g-i). These effects were not due to changes in physical activity after abGC depletion (Figure supplement 1a). Cessation of VGCV treatment in GFAP-TK mice enabled a 70% recovery of abGCs in the DG (Figure 1j,m) and complete recovery of abGC 3R-Tau+ axon intensity in the CA2 (Figure 1k,o). Coinciding with the recovery of adult neurogenesis, GFAP-TK animals regained the ability to discriminate between their mother and a novel mother (Figure 1i). These results reveal that abGCs play no role in “storing” developmental social memories, but instead support remote social memory retrieval, potentially through their projections to the CA2.

abGC projections to the CA2 play a time-limited role in the retrieval of remote developmental memories

To determine if developmental social memory retrieval requires activation of the abGC-CA2 circuit, we used a tamoxifen-inducible double transgenic mouse where Gi-DREADD expression was confined to abGCs in a temporally specific way (Nestin-cre:Gi). Nestin-cre littermates were used as single transgenic controls. Targeted CNO infusion in Nestin-cre:Gi mice enabled the inhibition of Gi-DREADD+ abGC axon terminals present in CA2. Tamoxifen-treated adult mice underwent behavioral testing at two post-injection time points to assess whether abGCs at different ages are involved in developmental social memory retrieval (4-6 and 10-12 weeks post-injection) (Figure 2a-c). Previous studies have shown that abGCs are highly excitable and exhibit enhanced synaptic plasticity between 4-6 weeks after their generation, properties that appear to be diminished by 8 weeks post-mitosis (Toni and Schinder, 2015). We found that Nestin-cre:Gi mice were able to discriminate between their mother and a novel mother when vehicle was

infused, but inhibition of this pathway after CNO infusion in CA2 prevented this ability (Figure 2e). These results were not related to differences in activity levels (Figure supplement 1b,c). Inhibition of projections from the same abGC cohort six weeks later (10-12-week-old abGCs) had no effect on Nestin-cre:Gi animals' ability to discriminate between their mother and a novel mother (Figure 2f). These findings suggest that abGCs are required for retrieving remote social memories when the cells are immature (4-6 weeks post-mitosis), but not when they are mature (10-12 weeks post-mitosis), presumably because a younger abGC cohort has taken over this function. An additional experiment explored if abGCs contribute to social memory consolidation (Figure 2g). Immature abGCs were silenced immediately after investigation of a novel adult mouse. When reintroduced to the now familiar adult mouse 6 hours later, after the effects of CNO had largely worn off, animals exhibited control-like social discrimination (Figure 2h), suggesting that abGC activity may not be required for social memory consolidation.

abGCs are necessary for differential network activity in the CA2 during exposure to novel versus familiar social stimuli

In the hippocampus, novelty detection, memory consolidation, and memory retrieval have been associated with the generation of high-frequency oscillations known as SWRs. SWRs coincide with replay and pre-play events that are believed to underlie learning and decision-making (Joo and Frank, 2018). Beyond its role in supporting spatial memory, SWR generation within the CA2 has been causally linked to social memory function (Oliva et al., 2020). The DG is known to influence SWR production (Bott et al., 2016), but no previous studies have investigated whether abGCs contribute to SWR generation in the CA2, or any CA subregion. Given our data showing that the abGC-CA2 circuit is important for the retrieval of developmental social memories, we hypothesized that abGCs might influence SWR generation in the CA2. In separate groups of Nestin-cre and Nestin-cre:Gi mice, we recorded neuronal oscillations in the CA2 with and without inhibition of 4-6-week-old abGCs. We found that SWR production is increased during social interaction, with more SWRs produced during novel mouse investigation, presumably during encoding social memories, than during familiar mouse investigation, presumably during retrieval of developmental social memories (Figure 3g-i). Inhibition of abGCs in the presence of a social stimulus altered several features of SWR production, including SWR frequency, peak amplitude, integral, and duration (Figure 3f-i – figure supplement 2b,c). Conversely, inhibition of 10-12-week-old abGCs had no effect on social novelty-induced

increases in CA2 SWRs, nor did it affect other features of SWR production (Figure 3m-r – figure supplement 2d,e). These findings suggest that 4-6 week-old abGCs, but not 10-12 week-old abGCs, are necessary for promoting appropriate SWR responses during social novelty exploration and developmental social memory retrieval. In an additional study, we investigated if CA2 SWRs were modulated by the presence of a nonsocial stimulus (an object) (Figure S3a). Somewhat suprisingly, CA2 SWR generation was suppressed upon exposure to a nonsocial stimulus (Figure supplement 3b). Inhibiting immature abGCs had little effect on SWR features in response to a nonsocial stimulus (Figure supplement 3c-f).

We next investigated abGC contributions to theta-gamma PAC, which is increased after exposure to social stimuli (Zhu et al., 2022) and has been linked to nonsocial memory retrieval (Tronel et al., 2015). We found that retrieval of a developmental social memory coincided with increased theta-mid gamma PAC, and that this increase was prevented after inhibition of 4-6 week-old abGCs (Figure 3j-l). Conversely, 4-6-week-old abGCs had no influence on CA2 oscillation power across theta, low gamma, and mid gamma frequency bands (Figure supplement 4a-f). Inhibition of a 10-12-week-old cohort of abGCs had no effect on the retrieval-induced increase in PAC (Figure 3s-u), suggesting that abGC influence on CA2 network activity is limited to a specific abGC age range. Taken together with our SWR results, these findings suggest that 4-6-week-old abGCs support CA2 network oscillations present during encoding and retrieval of social memories.

Discussion

Hippocampal CA2 plays an important role in supporting social recognition (Diethorn and Gould, 2023; Hitti and Siegelbaum, 2014; Laham et al., 2021; Smith et al., 2016), yet the contributions of the abGC projection to this region have remained uninvestigated. Here we show that ablation of abGCs impairs the retrieval of developmental social memories. Recovery of abGCs and their projections to CA2 restored the ability to demonstrate developmental social memory, revealing that abGCs support developmental social memory retrieval and not remote memory storage. Implementing a double transgenic mouse model, we found that chemogenetic inhibition of projections from 4-6-week-old abGCs to the CA2 prevents retrieval of a developmental social memory. This effect was not detected when inhibiting 10-12-week-old abGC projections, revealing that abGCs possess a time-sensitive ability to support retrieval of

developmental social memories. We next investigated if abGCs support developmental social memory retrieval via modulation of CA2 network activity. Inhibiting 4-6-week-old abGCs alters SWR generation and theta-mid gamma PAC in the CA2 region in a way that homogenizes network activity across novel and familiar social interactions. This impairment in network activity likely contributes to the inability to socially discriminate. These data suggest that abGCs contribute to the diversification of neuronal oscillatory states in the CA2 in the service of both recognizing social novelty and retrieving developmental social memories.

Materials and Methods

Animals

All animal procedures were approved by the Princeton University Institutional Animal Care and Use Committee and were in accordance with the National Research Council Guide for the Care and Use of Laboratory Animals. C57 male and female mice were obtained from Jackson laboratories and were used for immunolabeling. Transgenic mice expressing herpes simplex virus thymidine kinase (TK) under the GFAP promoter were bred in the Princeton Neuroscience Institute animal colony with founders provided by Dr. Heather Cameron at the National Institute of Mental Health for adult neurogenesis ablation studies. GFAP-TK mice were generated by crossbreeding CD1 male mice with heterozygous GFAP-TK female mice (Snyder et al., 2011). Nestin-CreERT2 and R26LSL-hM4Di single transgenic mice were obtained from Jackson labs and bred in the Princeton Neuroscience Institute as single or double transgenic mice for cannula implantation and electrophysiology experiments. PV-cre mice were obtained from Jackson labs and bred in the Princeton Neuroscience Institute to investigate abGC projections to CA2 PV+ interneurons. All studies used mixed-sex groups. Transgenic mice were genotyped by Transnetyx from ear punches at P15 using real-time PCR, separated from their dams at P21 and treated with VGCV or subjected to craniotomy for cannula implantation, or electrode implantation starting around P60. GFAP-TK mice were group housed by genotype and sex while single and double transgenic animals were group housed by sex only. Animals were housed in Optimice cages on a reverse 12/12 h light/dark cycle.

Behavioral testing

The direct social interaction test was used (Laham et al., 2021) to determine whether adult offspring were able to discriminate between a novel mother and their mother. To avoid the

confound of altered social preference during times of sexual receptivity, the estrous cycle was tracked in the mother and novel mother, and behavioral testing only occurred when stimulus mice were in diestrus (Cora et al., 2015). Adult TK, Nestin-cre, and Nestin-cre:Gi offspring underwent a social interaction test in which they directly interacted with the mother, or a novel mother (the novel mother was age-matched to the mother with similar reproductive experience). After a 1-hour delay spent in the home cage, mice were introduced to the stimulus animal not previously encountered for an additional five minutes. The order of stimulus exposure was counterbalanced in all tests. All behavioral tests were recorded, and a trained observer scored behavior testing under blind conditions. Testing apparatuses were cleaned with 70% ethanol after each trial. Bouts of investigation were characterized as direct sniffing of the stimulus mouse's anogenital region, body, and head.

An additional experiment explored abGC contributions to social memory consolidation. Nestin-cre and Nestin-cre:Gi mice were placed in a testing apparatus housing a novel adult mouse and were permitted to investigate for 5 minutes. Immediately after the conclusion of the test, mice received a systemic injection of Veh or 5 mg/kg CNO and were returned to the vivarium for 6 hours. At the conclusion of the 6-hour intertrial interval, mice were returned to the testing apparatus housing the stimulus mouse they had previously encountered and allowed to investigate for an additional 5 minutes. The use of a 6-hour intertrial interval ensured that CNO had minimal effects on abGC activity at the time of memory retrieval.

Surgical procedures

Mice were deeply anesthetized with isoflurane (2-3%) and placed in a stereotaxic apparatus (Kopf) under a temperature-controlled thermal blanket for all surgeries. The head was leveled using bregma, lambda, and medial-lateral reference points before virus injection, or implantation of either cannula or electrode was performed. PV-cre mice received bilateral injections of a cre-dependent mCherry AAV into CA2 (AP: -1.82, ML: +/-2.15, DV: -1.67) through a WPI nanofil 33 gauge beveled needle. Nestin-cre and Nestin-cre:Gi mice were bilaterally implanted with cannulae (Plastics One, Cat# C315GS-5/SP) targeting CA2. Dummy cannula (Plastics One, Cat# C315DCS5/SPC) were tightened inside guides prior to implantation. After lowering to the desired target region, cannula were secured in place using metabond followed by dental cement (Bosworth Trim). For CA2 recordings, Nestin-cre and Nestin-cre:Gi mice were implanted unilaterally with a custom-made 4-wire electrode array (Microprobes) into the right hemisphere

targeting CA2. Four bone screws were implanted into the skull with one screw on the contralateral hemisphere serving as ground. The ground wire was wrapped around the ground screw and covered with metallic paint to ensure maximum contact. Electrode implants were kept in place using metabond followed by dental cement (Bosworth Trim). Two weeks after surgeries, cannula mice were infused with either vehicle or clozapine-N-oxide (CNO) before being tested on behavioral tasks (see Behavioral testing); electrode mice received systemic injections of vehicle or CNO 30 min prior to electrophysiological recordings (see Electrophysiology recordings).

Drug treatments

Administration of the antiviral drug valganciclovir (VGCV) ablates adult neurogenesis in GFAP-TK animals. CD1 and GFAP-TK mice underwent behavioral testing at three time points. Animals first underwent testing prior to VGCV administration (VGCV-trial). After the first round of behavioral testing, VGCV was added to powdered rodent chow (227 mg of VGCV per kg chow) for six weeks. After six weeks of consuming VGCV chow, animals underwent behavioral testing for a second time (VGCV+ trial). At the conclusion of the VGCV+ trial, VGCV chow was removed from all cages and replaced with standard chow. After six weeks of standard chow consumption, animals underwent a third round of behavioral testing (VGCV-recovery). Mice were euthanized shortly after the third round of behavioral testing to assess the extent of adult neurogenesis recovery.

Cannula-implanted Nestin-cre and Nestin-cre:Gi mice underwent social discrimination testing (with novel mother and mother stimulus mice) twice, once after vehicle cannula infusion and once after CNO cannula infusion. The order of drug administration (vehicle or CNO) was counterbalanced across groups. Electrode-implanted mice underwent social discrimination testing with systemic vehicle or CNO administration. Mice were given a 48 hour minimum rest period between vehicle and CNO tests as previous studies have shown that DREADD manipulations of neurons are transient and return to baseline by 10-24 hours post-CNO injections (Alexander et al., 2009; Ray et al., 2011). 30 min prior to the first stimulus mouse exposure, test mice received vehicle or CNO cannula infusions. For cannula infusions, vehicle or 200 μl of CNO (2 μg/μl of CNO dissolved in DMSO suspended in saline) (Chang and Gean, 2019) was infused per hemisphere over 1 minute into CA2 using a syringe pump (Harvard

apparatus) mounted with a 1 μl syringe (Hamilton). The internal cannula remained in place for one additional minute after the infusion was completed to allow for diffusion of the drug.

Electrophysiology recordings

Local field potentials (LFPs) were recorded using a wireless head stage (TBSI, Harvard Biosciences). To habituate mice to the weight of the recording head stage, mice were connected to a custom head stage with equivalent weight while in the home cage for 10 min a day for five consecutive days. The behavioral testing paradigm consisted of a 3-minute baseline followed by a 5-minute social interaction period. Animals underwent this recording paradigm for both mother and novel mother trials. Vehicle or CNO was administered via IP injection 30 minutes before testing. In an additional experiment, Nestin-cre and Nestin-cre:Gi mice with CA2 electrodes were recorded during a 1-minute baseline followed by a 2-minute nonsocial object exposure trial. The nonsocial stimulus was a plastic toy animal of similar size to the mouse. Both baseline and nonsocial stimulus trials took place in an apparatus identical to that of the social stimulus experiments. The nonsocial stimulus trials were conducted after the conclusion of all social testing at the 4-6-week-old abGC time point. LFPs were recorded continuously throughout baseline and stimulus trials. The data were transmitted to a wireless receiver (Triangle Biosystems) and recorded using NeuroWare software (Triangle Biosystems).

Sharp wave-ripple analysis

All recordings were processed using Neuroexplorer software (Nex Technologies) and custom Python scripts (Laham and Zahn, 2023). For SWR analyses, continuous LFP data were notched at 60 Hz and band-pass filtered between 140 and 220 Hz. Signal underwent Hilbert transform before being z-scored. Using a custom Python script, SWRs were considered as events exceeding three standard deviations for a minimum of 15 ms. SWRs occurring within 15 ms of one another were merged into a single SWR event. SWR number was normalized to the respective baseline trial.

Phase-amplitude coupling analysis

Theta (4-12 Hz), low gamma (25-50 Hz), and mid gamma (50-100 Hz) oscillations were extracted from the raw LFP signal during social interaction using a custom Python script. Theta and mid-gamma recordings underwent a Hilbert transform, and theta phase and mid gamma analytic signal were stored. A custom python script identified periods of mid gamma recordings where analytic signal was 1.5 standard deviations above the mean. Only periods above 1.5

standard deviations were included in the analysis. PAC was quantified using a Modulation Index (Tort et al., 2010).

Histology

Mice were deeply anesthetized with Euthasol (Virbac) and were transcardially perfused with cold 4% paraformaldehyde (PFA). Extracted brains were postfixed for 48 h in 4% PFA at 4◦C followed by an additional 48 h in 30% sucrose at 4◦C for cryoprotection before being frozen in cryostat embedding medium at -80◦C. Hippocampal coronal sections (40 μm) were collected using a cryostat (Leica). Sections were blocked for 1.5 hr at room temperature in a PBS solution that contained 0.3% Triton X-100 and 3% normal donkey serum. Sections were then incubated overnight while shaking at 4◦C in the blocking solution that contained combinations of the following primary antibodies: mouse anti-three microtubule-binding domain tau protein (3R-Tau, 1:500, Millipore, Cat# 05-803), rabbit anti-Purkinje cell protein 4 (PCP4, 1:500, Sigma-Aldrich, Cat# HPA005792), rabbit anti-zinc transporter 3 (ZnT3, 1:500, Alomone labs, Cat# AZT-013). For 3R-Tau immunohistochemistry, sections were subjected to an antigen retrieval protocol that involved incubation in sodium citrate and citric acid buffer for 30 min at 80◦C prior to blocking solution incubation. Washed sections were then incubated for 1.5 hr at room temperature in secondary antibody solutions that contained combinations of the following secondaries: donkey anti-rat Alexa Fluor 568 (1:500, Abcam), donkey anti-mouse Alexa Fluor 568 or 647 (1:500, Invitrogen), or donkey anti-rabbit Alexa Fluor 488 (1:500, Invitrogen). Washed sections were then counterstained with Hoechst 33342 for 10 min (1:5,000 in PBS, Molecular Probes), mounted onto slides, and coverslipped with Vectashield (Vector labs). Slides were coded until completion of the data analysis. Sections through the ventral hippocampus from cannula and electrophysiology studies were stained for Hoechst 33342 in order to verify accurate cannula and electrode placement.

Optical intensity measurements

Z-stack images (0.5μm thickness) of the CA2 and corpus callosum were taken on a Leica SP8 confocal using LAS X software (version 35.6) and a 40x oil objective. The CA2 was defined by PCP4 labeling. Collected z-stack images were analyzed for optical intensity in Fiji (NIH). A background subtraction using a rolling ball radius (50 pixels) was applied to the image stacks. A region of interest (ROI) was drawn and the mean gray value was collected throughout the image stack. In the CA2, the ROI was confined to the stratum lucidum for 3R-Tau and ZnT3. The mean

gray value of the ROI was calculated for each z-slice and the maximum mean gray value for each z-stack was taken. The maximum of the CA2 ROI was divided by the maximum of the corpus callosum ROI for each section. Each brain's normalized intensity was the average of 3 sections.

Cell density and percentage measurements

The number of 3R-Tau+ cells was counted in the dorsal dentate gyrus of the hippocampus on 4 neuroanatomically matched sections using an Olympus BX-60 microscope with a 100x oil objective. The area measurements were collected using Stereo Investigator software (MBF). The density of 3R-Tau was determined by dividing the total number of positively labeled cells by the volume of the subregion (ROI area multiplied by 40 μm section thickness).

Statistical analyses

For histological analyses, data sets were analyzed using an unpaired two-tailed Student's t-test or Mann-Whitney U tests. For behavioral analyses involving two group comparisons, data sets were analyzed using either unpaired two-tailed Student's t-tests or a repeated measures two-way ANOVA, as appropriate. For behavioral analyses involving virus manipulations, data sets were analyzed using either a two-way ANOVA or a repeated measures three-way ANOVA, as appropriate. Bonferroni post hoc comparisons were used to follow up any significant main effects or interactions of the ANOVAs. Pearson's correlation coefficient test was used to analyze the association between theta power and social investigation times. Because electrophysiological measurements were taken from multiple electrodes within each mouse, these data were analyzed with linear mixed-effects ANOVAs using the lme4 package (Bates et al., 2015). The level of the measurement was explained by drug, virus, genotype, the three two-way interactions, the three-way interaction, and a random effect of mouse. Tukey post hoc comparisons were used to follow up any significant main effects or interactions using the emmeans package (Lenth, 2022). All data sets are expressed as the mean ± SEM on the graphs and statistical significance was set at $p < 0.05$ with 95% confidence. GraphPad Prism 9.2.0 (GraphPad Software), Excel (Microsoft), or R studio were used for statistical analyses. All graphs were prepared using GraphPad Prism 9.2.0 (GraphPad Software).

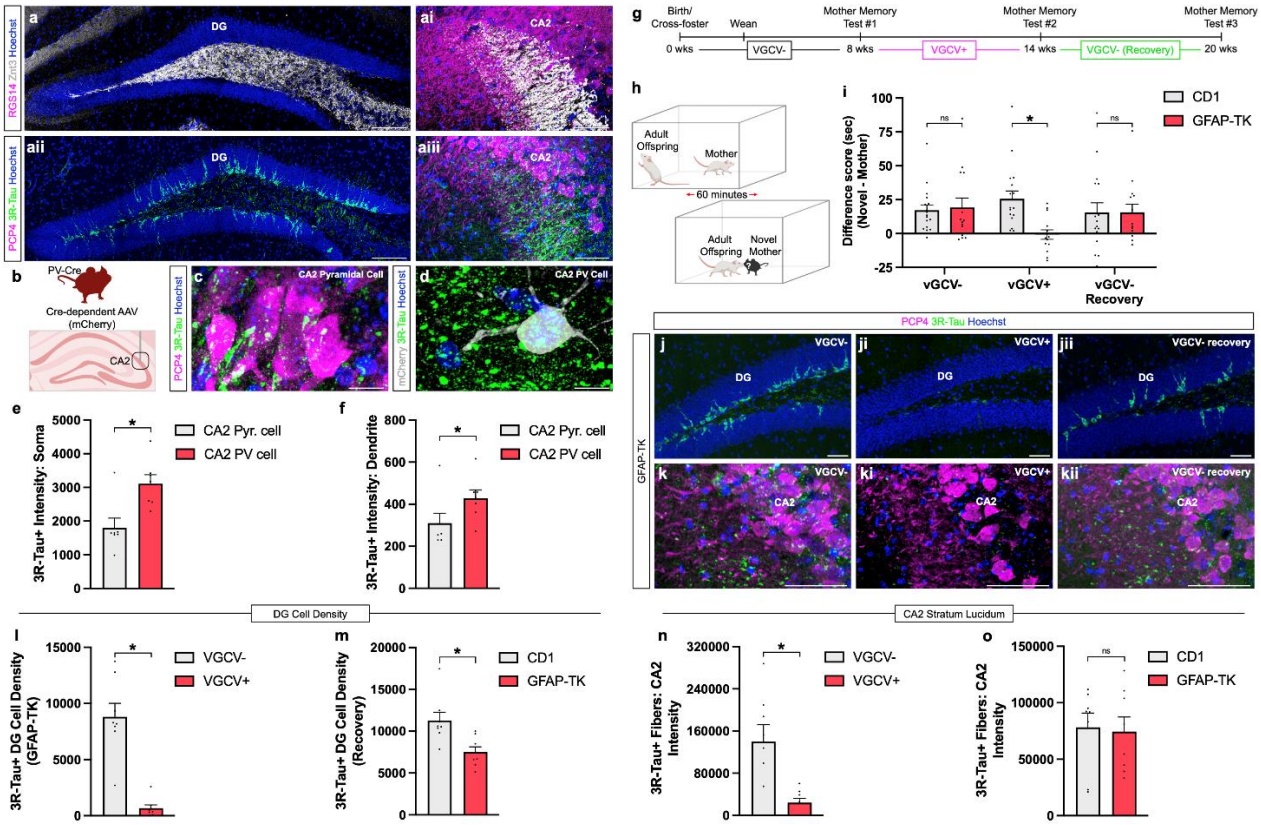

Figure 1: Adult-born neurons support retrieval of the earliest social memories.
a-aiii, Dentate gyrus granule cells, both mature (ZnT3+) and adult-born (3R-Tau+), send robust projections to CA2. **b**, Schematic showing injection of cre-dependent AAV (mCherry) targeting CA2 in PV-cre transgenic mice. **c**,**d**, abGC projections in close proximity to cell bodies and dendrites of CA2 PCP4+ pyramidal cells and mCherry+ PV+ interneurons. **e,f,** abGC fibers (3R-Tau+) in the CA2 are more abundant near the soma and dendrites of PV+ interneurons (mCherry+) than near the soma and dendrites of pyramidal cells (PCP4+). **g**, Timeline for behavioral experiment. **h**, Schematic demonstrating direct social interaction assay used at three experimental time points. **i,** Ablation of abGCs abolishes ability to retrieve memory of the mother (Drug x Genotype: p = 0.0074; vGCV+: p = 0.0021). After removing vGCV from rodent chow and allowing adult neurogenesis to recovery over the course of six weeks, animals regain the ability to retrieve the memory of the mother (p > 0.999). **j-kii,** Hippocampal adult neurogenesis at three different drug time points. VGCV administration produces a dramatic loss of **l**, abGCs (3R-Tau+ cells) in DG (p < 0.0001) and **n,** 3R-Tau+ fibers in CA2 stratum lucidum (p = 0.0036). Six weeks after removing vGCV from the rodent chow, DG abGC number, **m,** undergoes a 70% recovery (p = 0.0062), and, **o,** 3R-Tau+ fibers present in CA2 stratum lucidum undergo a complete recovery (p = 0.8389). $*p$ < 0.05, bars represent mean + SEM. Scale bars = 200 μm for **a-aiii** and **j-kii**; 20 μm for **c**,**d**. ns = not significant.

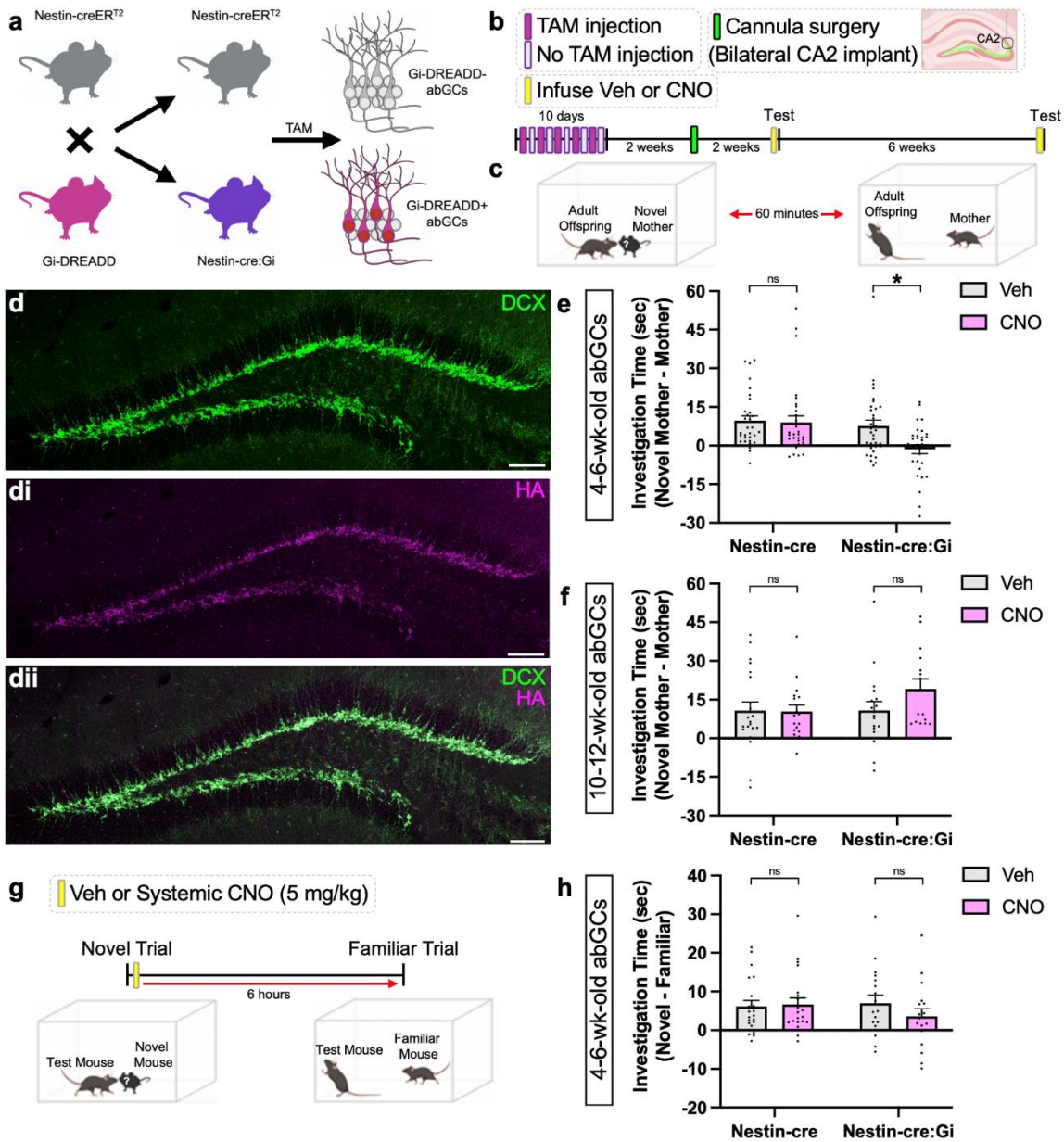

Figure 2: Inhibiting 4-6-week-old abGC projections to CA2 prevents retrieval of the earliest social memories.

a, Schematic of breeding to produce Nestin-cre:Gi double transgenic offspring. **b,** Timeline outlining tamoxifen administration, cannula implantation, and behavioral testing. **c,** Schematic demonstrating direct social interaction testing. **d-dii,** histology depicting 4-6-week-old Gi-DREADD+ abGCs in the DG. **e,** Inhibiting 4-6-week-old abGC projections to CA2 with CNO prevents retrieval of the memory of the mother (Genotype x Drug: $p = 0.0487$; Nestin-cre:Gi Veh-CNO: $p = 0.0057$). **f,** Inhibiting 10-12-week-old abGC projections to CA2 does not influence retrieval of the earliest social memories (Genotype x Drug: $p = 0.2008$). **g,** Schematic for experiment assessing abGC contributions to social memory consolidation. Systemic inhibition of abGCs during memory consolidation has no significant effect on social memory (Genotype x Drug: $p = 0.2730$). $*p < 0.05$, bars represent mean + SEM. Scale bars = 200 µm. ns = not significant.

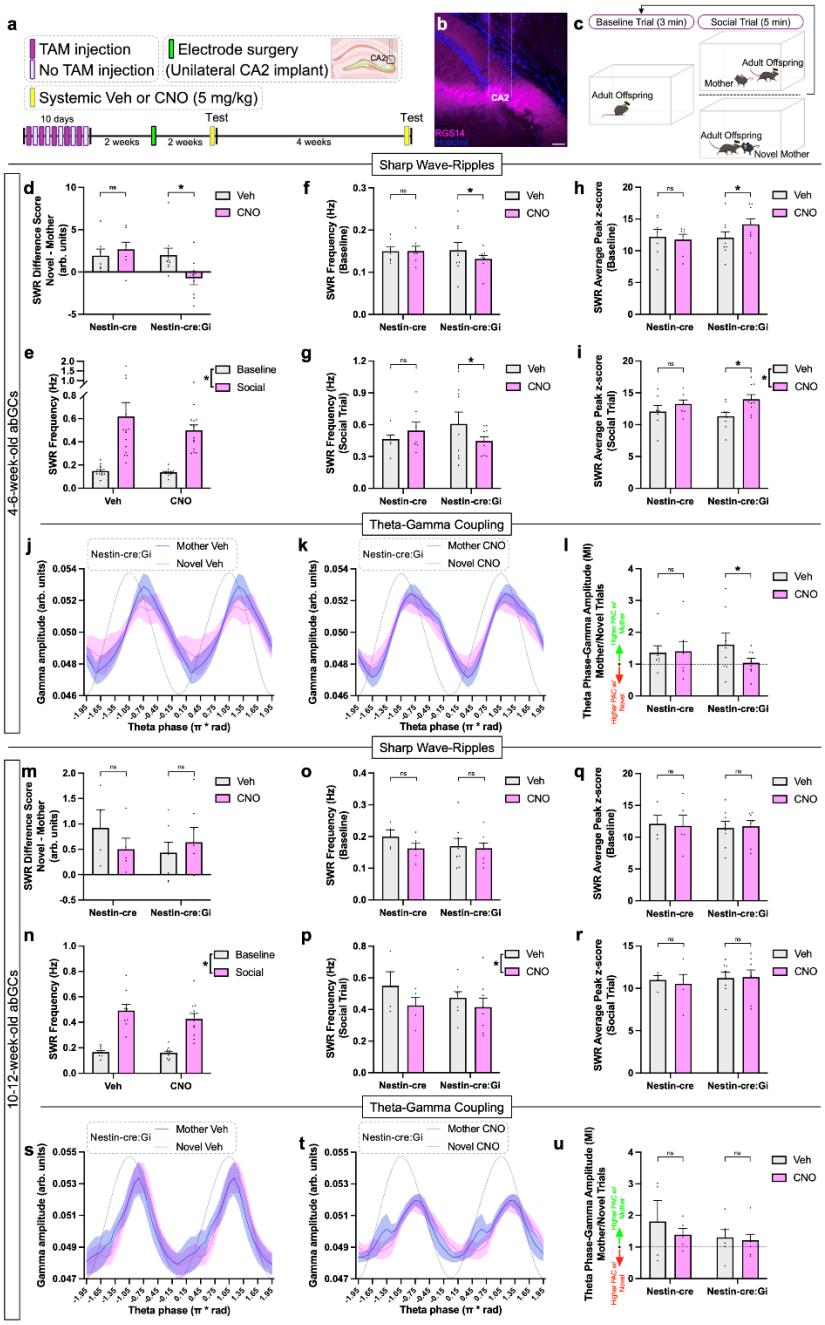

Figure 3: Adult-born neurons influence CA2 network activity associated with developmental social memory retrieval.

a, Timeline of experiment demonstrating tamoxifen injection schedule and electrode implantation in CA2. **b,** Histology demonstrating accuracy of electrode placement. **c,** Schematic of electrophysiological recordings during baseline and social trials. **d,** Inhibiting 4-6-week-old abGCs with CNO prevents characteristic SWR production patterns present during encoding vs retrieval of social memories (Genotype x Drug: $p < 0.0001$; Nestin-cre:Gi CNO Novel-Mother: $p < 0.0101$). **e,** CA2 SWR frequency is increased during social interactions, regardless of stimulus identity (Stimulus: $p < 0.0001$). Inhibiting 4-6-week-old abGCs reduces **f** baseline (Genotype x Drug: $p = 0.0622$; Nestin-cre:Gi Veh-CNO: $p = 0.0308$) and **g** social trial SWR production (Genotype x

Drug: $p < 0.0001$; Nestin-cre:Gi Veh-CNO $p = 0.0018$), and increases SWR peak amplitude during **h** baseline (Genotype x Drug: $p = 0.0147$; Veh-CNO: $p = 0.0133$) and **i** social interaction trials (Genotype x Drug: $p = 0.0559$; Nestin-cre:Gi Veh-CNO: $p < 0.0001$). **j**,**k,** Graphs demonstrating mid gamma amplitude modulation across theta phases in Nestin-cre:Gi mice. **l,** Inhibiting 4-6-week-old abGCs abolishes the increase in theta-mid gamma PAC present during retrieving the memory of the mother (Genotype x Drug: $p = 0.0329$; Nestin-cre:Gi Veh-CNO: $p = 0.0219$). **m,** Inhibiting 10-12-week-old abGCs has no influence on characteristic SWR production patterns present during encoding vs retrieval of social memories (Genotype x Drug: $p = 0.2781$). **n,** CA2 SWR frequency is increased during social interactions, regardless of stimulus familiarity (Stimulus: $p < 0.0001$). Inhibiting 10-12-week-old abGCs has no influence on **o** baseline (Genotype x Drug: $p = 0.4612$) or **p** social trial SWR production (Genotype x Drug: $p = 0.5702$), and no influence on SWR peak amplitude during **q** baseline (Genotype x Drug: $p = 0.8125$) and **r** social interaction trials (Genotype x Drug: $p = 0.7635$). **s**,**t,** Graphs demonstrating mid gamma amplitude modulation across theta phases in Nestin-cre:Gi mice. **u,** Inhibiting 10-12-week-old abGCs has no influence on theta-mid gamma PAC while retrieving the memory of the mother (Genotype x Drug: $p = 0.6153$). $*p < 0.05$, bars represent mean + SEM. Scale bars = 200 μm. ns = not significant.

References

Alexander, G.M., Rogan, S.C., Abbas, A.I., Armbruster, B.N., Pei, Y., Allen, J.A., Nonneman, R.J., Hartmann, J., Moy, S.S., Nicolelis, M.A., McNamara, J.O., Roth, B.L. Remote control of neuronal activity in transgenic mice expressing evolved G protein-coupled receptors. Neuron. 63, 27-39 (2009).

Bates, D., Mächler, M., Bolker, B., Walker,S. Fitting linear mixed-effects models using lme4.J. Stat. Softw. 67,1–48 (2015).

Bott, J.B., Muller, M.A., Jackson, J., Aubert, J., Cassel, J.C., Mathis, C., Goutagny, R. Spatial reference memory is associated with modulation of theta-gamma coupling in the dentate gyrus. Cereb Cortex. 26, 3744-3753 (2016).

Brown, L.Y., Alexander, G.M., Cushman, J., Dudek, S.M. Hippocampal CA2 organizes CA1 slow and fast γ oscillations during novel social and object interaction. eNeuro. 7, ENEURO.0084-20.2020 (2020).

Chang, C.H., Gean, P.W. The ventral hippocampus controls stress-provoked impulsive aggression through the ventromedial hypothalamus in post-weaning social isolation mice. Cell Rep. 28, 1195–1205.e3 (2019).

Colgin, L.L. Theta-gamma coupling in the entorhinal-hippocampal system. Curr Opin Neurobiol. 31, 45-50 (2015).

Cope, E.C., Waters, R.C., Diethorn, E.J., Pagliai, K.A., Dias, C.G., Tsuda, M., Cameron, H.A., Gould, E. Adult-born neurons in the hippocampus are essential for social memory maintenance. eNeuro. 7, ENEURO.0182-20.2020 (2020).

Cora, M.C., Kooistra, L., Travlos, G. Vaginal cytology of the laboratory rat and mouse: review and criteria for the staging of the estrous cycle using stained vaginal smears. Toxicol Pathol. 43,776-93 (2015).

Diethorn, E.J., Gould, E. Postnatal development of hippocampal CA2 structure and function during the emergence of social recognition of peers. Hippocampus. 33, 208-222 (2023).

Fernández-Ruiz, A., Oliva, A., Fermino de Oliveira, E., Rocha-Almeida, F., Tingley, D., Buzsáki, G. Long-duration hippocampal sharp wave ripples improve memory. Science. 364, 1082-1086 (2019).

Fivush, R. The development of autobiographical memory. Annu Rev Psychol. 62, 559-82 (2011)

Hitti, F.L., Siegelbaum, S.A. The hippocampal CA2 region is essential for social memory. Nature. 508, 88-92 (2014).

Joo, H.R., Frank, L.M. The hippocampal sharp wave-ripple in memory retrieval for immediate use and consolidation. Nat Rev Neurosci. 19, 744-757 (2018).

Kohara, K., Pignatelli, M., Rivest, A.J., Jung, H.Y., Kitamura, T., Suh, J., Frank, D., Kajikawa, K., Mise, N., Obata, Y., Wickersham, I.R., Tonegawa, S. Cell type-specific genetic and optogenetic tools reveal hippocampal CA2 circuits. Nat Neurosci. 17, 269-79 (2014).

Laham, B. J., Zahn, E. einaraz/SharpWaveRipple: V0.0.2 (v0.0.2). Zenodo. https://doi.org/10.5281/zenodo.7592606 (2023).

Laham, B.J., Diethorn, E.J., Gould, E. Newborn mice form lasting CA2-dependent memories of their mothers. Cell Rep. 34,108668 (2021).

Lenth, R. emmeans: Estimated Marginal Means, aka Least-Squares Means_. R package version 1.7.5, https://CRAN.R-project. org/package=emmeans (2022).

Llorens-Martín, M., Jurado-Arjona, J., Avila, J., Hernández, F. Novel connection between newborn granule neurons and the hippocampal CA2 field. Exp Neurol. 263, 285-92 (2015).

McHugh, S.B., Lopes-Dos-Santos, V., Gava, G.P., Hartwich, K., Tam, S.K.E., Bannerman, D.M., Dupret, D. Adult-born dentate granule cells promote hippocampal population sparsity. Nat Neurosci. 25, 1481-1491 (2022).

Meier, K., Merseburg, A., Isbrandt, D., Marguet, S.L., Morellini, F. Dentate gyrus sharp waves, a local field potential correlate of learning in the dentate gyrus of mice. J Neurosci. 40, 7105-7118 (2020).

Oliva, A., Fernández-Ruiz, A., Leroy, F., Siegelbaum, S.A. Hippocampal CA2 sharp-wave ripples reactivate and promote social memory. Nature. 587, 264-269 (2020).

Pereira-Caixeta, A.R., Guarnieri, L.O., Medeiros, D.C., Mendes, E.M.A.M., Ladeira, L.C.D., Pereira, M.T., Moraes, M.F.D., Pereira, G.S. Inhibiting constitutive neurogenesis compromises long-term social recognition memory. Neurobiol Learning Mem 155, 92-103 (2018).

Ray, R.S., Corcoran, A.E., Brust, R.D., Kim, J.C., Richerson, G.B., Nattie, E., Dymecki, S.M. Impaired respiratory and body temperature control upon acute serotonergic neuron inhibition. Science. 333, 637-42 (2011).

Restivo, L., Niibori, Y., Mercaldo, V., Josselyn, S.A., Frankland, P.W. Development of adult-generated cell connectivity with excitatory and inhibitory cell populations in the hippocampus. J Neurosci. 35, 10600-12 (2015).

Schaal, B., Saxton, T.K., Loos, H., Soussignan, R., Durand, K. Olfaction scaffolds the developing human from neonate to adolescent and beyond. Philos Trans R Soc Lond B Biol Sci. 375, 20190261 (2020).

Smith, A.S., Williams Avram, S.K., Cymerblit-Sabba, A., Song, J., Young, W.S. Targeted activation of the hippocampal CA2 area strongly enhances social memory. Mol Psychiatry. 21, 1137-44 (2016).

Snyder, J.S., Soumier, A., Brewer, M., Pickel, J., Cameron, H.A. Adult hippocampal neurogenesis buffers stress responses and depressive behaviour. Nature. 476, 458-61 (2011).

Toni, N., Schinder, A.F. Maturation and functional integration of new granule cells into the adult hippocampus. Cold Spring Harb Perspect Biol. 8(1), a018903 (2015).

Tort, A.B., Komorowski, R., Eichenbaum, H., Kopell, N. Measuring phase-amplitude coupling between neuronal oscillations of different frequencies. J Neurophysiol. 104, 1195-210 (2010).

Tronel, S., Charrier, V., Sage, C., Maitre, M., Leste-Lasserre, T., Abrous, D.N. Adult-born dentate neurons are recruited in both spatial memory encoding and retrieval. Hippocampus. 25, 1472-9 (2015).

Vivekananda, U., Bush, D., Bisby, J.A., Baxendale, S., Rodionov, R., Diehl, B., Chowdhury, F.A., McEvoy, A.W., Miserocchi, A., Walker, M.C., Burgess, N. Theta power and theta-gamma coupling support long-term spatial memory retrieval. Hippocampus.31, 213-220 (2021).

Wenzel, H.J., Cole, T.B., Born, D.E., Schwartzkroin, P.A., Palmiter, R.D. Ultrastructural localization of zinc transporter-3 (ZnT-3) to synaptic vesicle membranes within mossy fiber boutons in the hippocampus of mouse and monkey. Proc Natl Acad Sci U S A. 94, 12676-81 (1997).

Zhu, N., Zhang, Y., Xiao, X, Wang, Y., Yang, J., Colgin, L.L., Cheng, C. Hippocampal oscillatory dynamics in freely behaving rats during exploration of social and non-social stimuli. Cogn Neurodyn (2022).

Figure Supplements

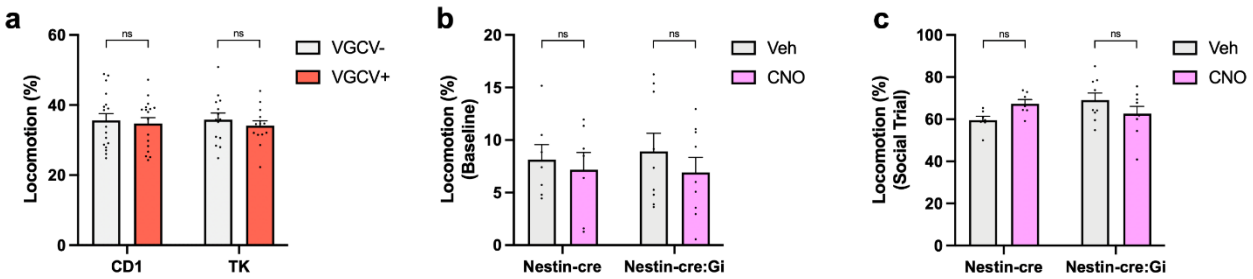

Figure Supplement 1: VGCV or CNO administration does not alter locomotion during social interaction.

a, GFAP-TK mice display normal locomotion during social interaction after six weeks of VGCV administration (Genotype x Drug: $p = 0.8154$). CNO administration has no effect on locomotion during **b** baseline (Genotype x Drug: $p = 0.7019$) or **c** social stimulus trials (Genotype x Drug: $p = 0.1171$) in Nestin-cre and Nestin-cre:Gi mice. Bars represent mean + SEM. ns = not significant.

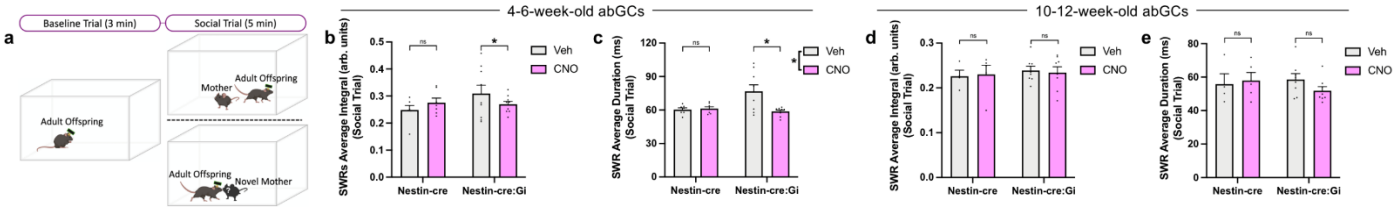

Figure Supplement 2: 4-6-week-old abGCs influence multiple features of CA2 SWRs.
a, Schematic of electrophysiological recordings during baseline and social trials during the 4-6-week-old abGC timepoint. **b,** Silencing 4-6-week-old abGCs reduces average CA2 SWR integral (Genotype x Drug: $p = 0.0004$; Nestin-cre:Gi Veh-CNO: $p = 0.0099$). **c**, Silencing 4-6-week-old abGCs reduces average CA2 SWR duration (Genotype x Drug: $p < 0.0001$; Nestin-cre:Gi Veh-CNO: $p < 0.0001$; Drug: $p < 0.0001$). **d**, Silencing 10-12-week-old abGCs reduces has no effect on average CA2 SWR integral but a significant interaction is observed (Genotype x Drug: $p = 0.0469$; Nestin-cre:Gi Veh-CNO: $p = 0.7457$). **e**, Silencing 10-12-week-old abGCs does not reduce average CA2 SWR duration but a significant interaction is observed (Genotype x Drug: $p = 0.00389$; Nestin-cre:Gi Veh-CNO: $p = 0.1439$). $*p < 0.05$, bars represent mean + SEM. ns = not significant.$*p < 0.05$, bars represent mean + SEM. ns = not significant.

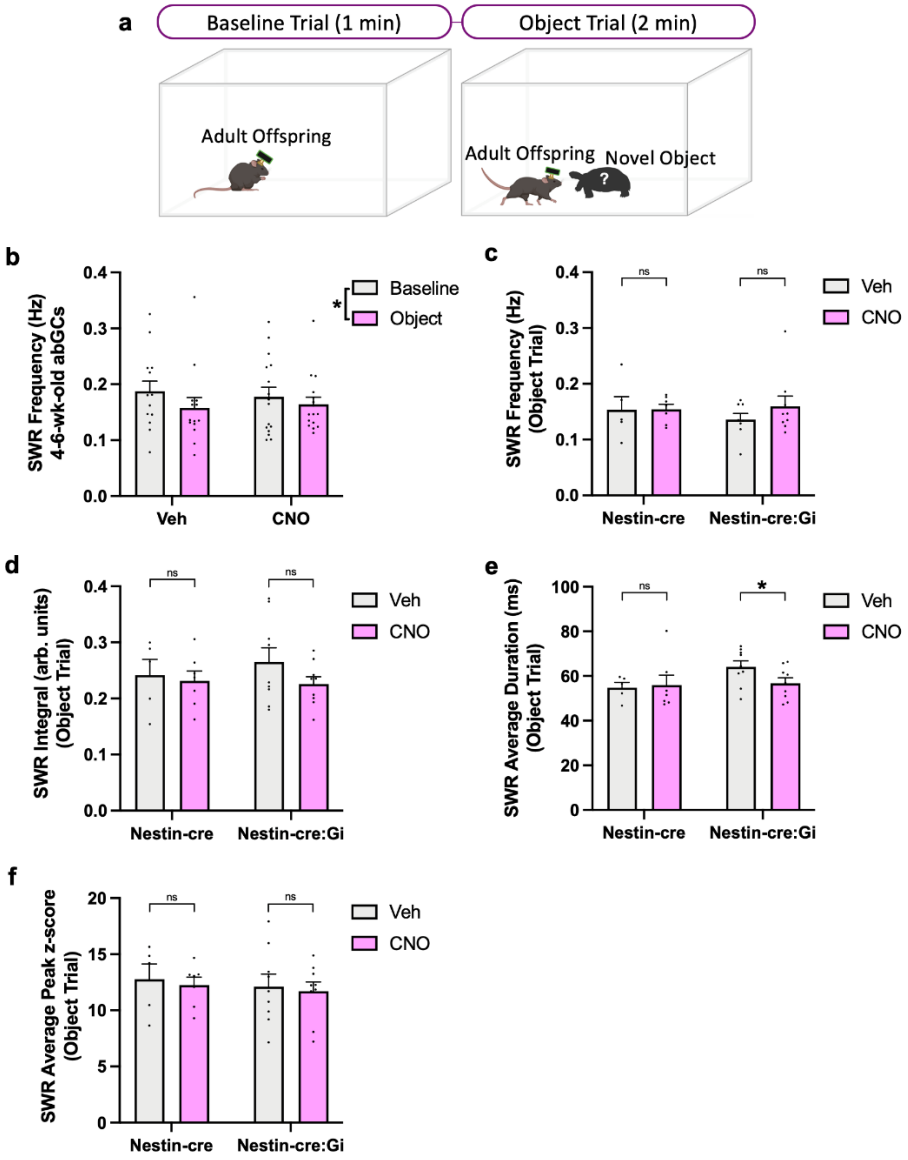

Figure Supplement 3: Nonsocial stimuli suppress CA2 SWR frequency.
a, Schematic of electrophysiological recordings during baseline and exposure to nonsocial object (plastic toy animal) trials during the 4-6-week-old abGC timepoint. **b**, Nonsocial stimuli slightly inhibit CA2 SWR frequency (Stimulus: $p = 0.0095$). **c**, Silencing 4-6-week-old abGCs has no influence on CA2 SWR frequency during object exposure (Genotype x Drug: $p = 0.3806$), **d** average integral (Genotype x Drug: $p = 0.2027$), and **f** peak z-score (Genotype x Drug: $p = 0.987$). **e**, Silencing 4-6-week-old abGCs reduces average SWR duration during object trials (Genotype x Drug: $p = 0.00585$; Nestin-cre:Gi Veh-CNO: $p = 0.0094$). $*p < 0.05$, bars represent mean + SEM. ns = not significant.

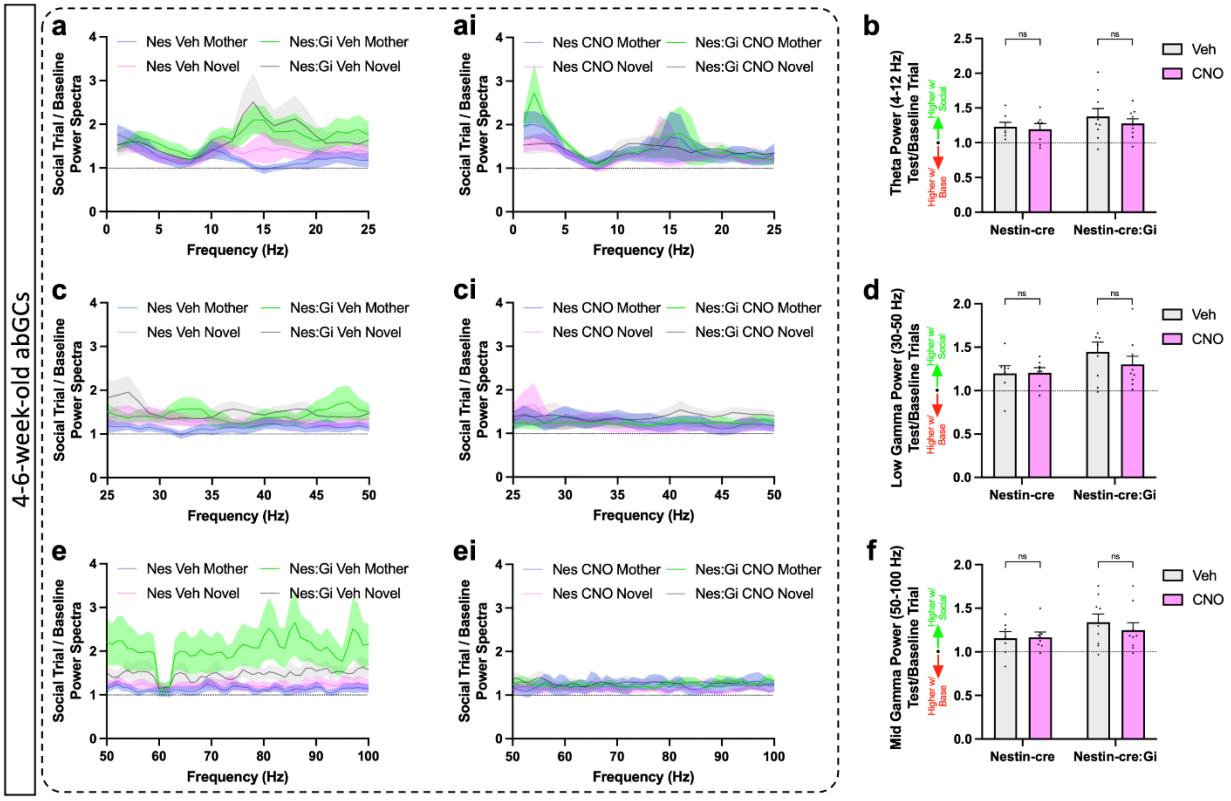

Figure Supplement 4: 4-6-week-old abGCs do not influence theta and gamma power during social interaction.

a,**ai**,**c**,**ci**,**e**,**ei**, Normalized power spectra graphs (Social stimulus/baseline). **b**, Silencing 4-6-week-old abGCs has no influence on theta power (Genotype x Drug: p = 0.6387). **d**, Silencing 4-6-week-old abGCs has no influence on low gamma power (Genotype x Drug: p = 0.3868). **f**, Silencing 4-6-week-old abGCs has no influence on mid gamma power (Genotype x Drug: p = 0.5478). Bars represent mean +/- SEM for **a**,**ai**,**c**,**ci**,**e**,**ei**; + SEM for **b**,**d**,**e**. ns = not significant.